Econometrics Journal (2019), volume **00**, pp. S.1–S.10.
Article No. ectj??????

Probabilistic Forecasting of Bubbles and Flash Crashes: Online Supplement

Anurag Banerjee[†], Guillaume Chevillon[‡] and Marie Kratz[⋆]

[†] *Durham Business School*
E-mail: a.n.banerjee@durham.ac.uk
[‡] *ESSEC Business School (Corresponding author)*
E-mail: chevillon@essec.edu
[⋆] *ESSEC Business School, CREAR*
E-mail: kratz@essec.edu
Received: 24 July 2019

Summary This online supplement records additional simulations, empirical applications and technical proofs.

S.1. SIMULATIONS OF PREDICTIVE PROBABILITIES

To study the patterns generated by predictive probabilities, we simulate, using 10^5 Monte Carlo replications, the values of $\pi_{t,h}(\gamma)$ obtained in Corollary (3.1) for $\gamma = 1.05$ and $\alpha = .8$. We consider $(\phi, \lambda) \in \{-1, 0, 1\} \times \{0, 5, 1, 2, 3\}$, and $h \in \{1, 6, 24\}$. In Figure S.1, we report simulated $\pi_{t,h}(\gamma)$ for a large sample size $T = 1000$ where $900 \leq t \leq 1000$. Figure S.2 records similar simulations for a smaller sample size $T = 200$ and we let $100 \leq t \leq 200$.

When $\phi = -1$ and for the range of (λ, h) considered, both figures report probabilities, with $\gamma > 1$, that hover below .50 and that decrease with h since the latter impacts positively the variance of conditional forecasts. Probabilities reported in Figure S.1 hardly vary with t, which shows that they are obtained from the ergodic distributions of the weakly stationary process. This is not the case when γ is time varying (e.g. a risk free rate) or for the smaller sample size reported in Figure S.2 where predictive probabilities tend to decrease as t increases.

For positive values of ϕ, the probabilities processes reported in Figure S.1 tend to be more dispersed as of function λ and get closer to 0.5 as λ and h increases. They are also more stable as a function of t for larger values of λ. In the relatively large sample considered in the figure, the predictive probabilities are always below .5 except when $\phi = 1$ and $h = 24$. By contrast, in the smaller sample size recorded in Figure S.2, $\pi_{t,h}(\gamma) > .5$ for smaller values of h when $\phi > 0$. This reflects the larger $\mathsf{E}\left(\rho_t^2\right)$ induced by the smaller T. Notice also that for so small a sample, the probabilities exhibit trending patterns as function of t.

S.2. ADDITIONAL EMPIRICAL APPLICATIONS

Figure S.3 considers the logarithm of the S&P 500 index since the early 1950s with $\gamma = 1.004$, which corresponds to an annual rate of growth of 5% – approximately the long run nominal growth of the economy. Throughout the sample, $\widehat{\pi}_{t,h}^{\min}(\gamma) < 0.5$ yet close to it (a random walk yields zero probability of a bubble according to our local-asymptotic

definition but $\Pr(y_{t+h}/y_t > 1|\mathcal{I}_t) = 0.5$ for t finite and $h \geq 1$), and $\widehat{\pi}_{t,h}^{\max}$ is strictly less than unity over the first two thirds of the sample, with $\widehat{\pi}_{t,h}^{med}(\gamma)$ close to 0.66. $\widehat{\pi}_{t,h}^{\max}(\gamma)$ increases over the sample to stabilize at 1, reflecting the growth of the data which does not preclude the possibility of explosive growth.

Comparable results are reported in Figure S.4 for the logarithm of the long term interest rates since the early 1960s with $\gamma = 1$. We notice the stability of the estimated probabilities. The main difference with the previous figure is that since the interest rate reverts towards the end of the sample to the values observed at the beginning, minimum and maximum probabilities shift downwards, with $\widehat{\pi}_{t,h}^{\max}(\gamma) < 1$, towards the end of the sample, which widens the range of predictive probabilities.

S.3. TECHNICAL PROOFS

S.3.1. Proof of the Lindeberg Condition in Lemma C.1 when $c < 0$.

We let $\xi_t = T^{-\frac{1+\alpha}{2}} y_{t-1}^2 (\rho_t - \rho)$ and prove that for all $\varepsilon > 0$, $\sum_{t=1}^{T} \mathsf{E}_{\mathcal{F}_{t-1}} \left(\xi_t^2 1_{\{|\xi_t| > \varepsilon\}}\right) \xrightarrow{p} 0$ as $T \to \infty$. where $\frac{\lambda^2}{T^{1+\alpha}} \sum_{t=1}^{T} y_{t-1}^4 \xrightarrow{p} \frac{3\lambda^2\sigma_\eta^4}{4c^2}$. Conditional expectations are based on the filtration $\mathcal{F}_{t-1} = \{y_0, (u_{t-j}, \eta_{t-j})\}_{j\geq 1}$.

Since we have

$$\begin{aligned}\sum_{t=1}^{T} \mathsf{E}_{\mathcal{F}_{t-1}} \left(\xi_t^2 1_{\{|\xi_t|>\varepsilon\}}\right) &= \frac{1}{T^{1+\alpha}} \sum_{t=1}^{T} y_{t-1}^4 \mathsf{E}_{\mathcal{F}_{t-1}} \left[(\rho_t - \rho)^2 1_{\left\{\left|y_{t-1}^2(\rho_t-\rho)\right| > \varepsilon T^{\frac{1+\alpha}{2}}\right\}}\right] \\ &\leq \max_{1\leq t\leq T} \mathsf{E}_{\mathcal{F}_{t-1}} \left[(\rho_t - \rho)^2 1_{\left\{\left|y_{t-1}^2(\rho_t-\rho)\right| > \varepsilon T^{\frac{1+\alpha}{2}}\right\}}\right] \frac{1}{T^{1+\alpha}} \sum_{t=1}^{T} y_{t-1}^4,\end{aligned}$$

it is enough to show that $\max_{1\leq t\leq T} \mathsf{E}_{\mathcal{F}_{t-1}} \left((\rho_t - \rho)^2 1_{\left\{\left|y_{t-1}^2(\rho_t-\rho)\right| > \varepsilon T^{\frac{1+\alpha}{2}}\right\}}\right) \xrightarrow{p} 0$ for all ε. By Assumption B, and for some $\nu > 2$, Hölder's inequality, for $r_1 = 2$ and $r_2 = 2$ with $r_1^{-1} + r_2^{-1} = 1$, together with Chebyshev's inequality imply that

$$\begin{aligned}&\mathsf{E}_{\mathcal{F}_{t-1}} \left((\rho_t - \rho)^2 1_{\left\{\left|y_{t-1}^2(\rho_t-\rho)\right| > \varepsilon T^{\frac{1+\alpha}{2}}\right\}}\right) \\ &\leq \mathsf{E}_{\mathcal{F}_{t-1}} \left((\rho_t - \rho)^{2r_1}\right)^{\frac{1}{r_1}} \mathsf{E}_{\mathcal{F}_{t-1}} \left(1_{\left\{\left|y_{t-1}^2(\rho_t-\rho)\right| > \varepsilon T^{\frac{1+\alpha}{2}}\right\}}\right)^{\frac{1}{2}} \\ &= \mathsf{E}_{\mathcal{F}_{t-1}} \left((\rho_t - \rho)^4\right) \mathsf{P}_{\mathcal{F}_{t-1}} \left(\left|y_{t-1}^2(\rho_t - \rho)\right| > \varepsilon T^{\frac{1+\alpha}{2}}\right)^{\frac{1}{2}} \\ &= \mathsf{E}\left((\rho_t - \rho)^4\right) \mathsf{P}_{\mathcal{F}_{t-1}} \left(\left|y_{t-1}^2(\rho_t - \rho)\right| > \varepsilon T^{\frac{1+\alpha}{2}}\right)^{\frac{1}{2}} \\ &\leq \mathsf{E}\left((\rho_t - \rho)^4\right) \left[\frac{\mathsf{E}_{\mathcal{F}_{t-1}}\left(y_{t-1}^4(\rho_t - \rho)^4\right)}{\varepsilon^2 T^{(1+\alpha)}}\right]^{\frac{1}{2}} \\ &= \left[\frac{6\lambda^2}{T^\alpha} + O\left(T^{-2\alpha}\right)\right] \sqrt{\frac{\frac{6\lambda^2}{T^\alpha} + O\left(T^{-2\alpha}\right)}{\varepsilon^2}} \frac{y_{t-1}^2}{T^{(1+\alpha)/2}}.\end{aligned}$$

Now,

$$\max_{1\leq t\leq T}\frac{y_{t-1}^2}{T^{5\alpha/2}T^{(1+\alpha)/2}}=\frac{\left(\max_{1\leq t\leq T}\left|\frac{y_{t-1}}{T^{\alpha/2}}\right|\right)^2}{T^{3\alpha/2}T^{(1+\alpha)/2}},$$

with

$$\max_{1\leq t\leq T}\left|\frac{y_{t-1}}{T^{\alpha/2}}\right|\leq\sup_{s\in[0,T^{1-\alpha}]}\left|\frac{y_{\lfloor T^{\alpha}s\rfloor}}{T^{\alpha/2}}-K_{\phi,\lambda}\left(s\right)\right|+\sup_{s>0}\left|K_{\phi,\lambda}\left(s\right)\right|=O_p\left(1\right),$$

by Proposition 2.1, and using an equivalent of Lemma 2.1 and Proposition A.2 of PM. The result follows.

S.3.2. Neglecting R_{0T}, R_{0T}^* and $R_{0T}^\times$ in Proof of Proposition 4.1.

We collect here the proofs that R_{0T}, R_{0T}^* and $R_{0T}^\times$ can be neglected in the expressions where they appear in the proofs above. They are defined as

$$\begin{aligned}
R_{0T}&=\sum_{t=1}^{T}y_t^2-\left[\sum_{k=1}^{\lfloor\kappa_T\rfloor}e^{\frac{2\phi}{T^\alpha}k+\frac{2\lambda}{T^{\alpha/2}}U_k}\right]\left[\sum_{i=1}^{\lfloor\kappa_T\rfloor}e^{-\frac{\phi}{T^\alpha}i-\frac{\lambda}{T^{\alpha/2}}U_i}\eta_i\right]^2,\\
R_{0T}^*&=\sum_{t=1}^{T}y_{t-1}\nu_t-\left[\sum_{k=1}^{\lfloor\kappa_T\rfloor}e^{\frac{\phi}{T^\alpha}k+\frac{\lambda}{T^{\alpha/2}}U_k}\nu_k\right]\left[\sum_{i=1}^{\lfloor\kappa_T\rfloor}e^{-\frac{\phi}{T^\alpha}i-\frac{\lambda}{T^{\alpha/2}}U_i}\eta_i\right],\\
R_{0T}^\times&=\sum_{t=1}^{T}y_{t-1}^2\nu_t-\left[\sum_{k=1}^{\lfloor\kappa_T\rfloor}e^{\frac{2\phi}{T^\alpha}k+\frac{2\lambda}{T^{\alpha/2}}U_k}\nu_k\right]\left[\sum_{i=1}^{\lfloor\kappa_T\rfloor}e^{-\frac{\phi}{T^\alpha}i-\frac{\lambda}{T^{\alpha/2}}U_i}\eta_i\right]^2.
\end{aligned}$$

We use the fact that $\kappa_T=T^\alpha\left\lfloor T^{1-\alpha}\right\rfloor=O\left(T\right)$ and

$$T-\lfloor\kappa_T\rfloor=T-\left\lfloor T-T^\alpha\left(T^{1-\alpha}-\left\lfloor T^{1-\alpha}\right\rfloor\right)\right\rfloor=O\left(T^\alpha\right).\tag{S.1}$$

In the following, we start with the case of R_{0T}^* as it is the simplest in terms of notation.

S.3.2.1. Case of R_{0T}^* First, write

$$\begin{aligned}
R_{0T}^*=&\left[\sum_{k=\lfloor\kappa_T\rfloor+1}^{T}e^{\frac{\phi}{T^\alpha}k+\frac{\lambda}{T^{\alpha/2}}U_k}\nu_k\right]\left[\sum_{i=1}^{T}e^{-\frac{\phi}{T^\alpha}i-\frac{\lambda}{T^{\alpha/2}}U_i}\eta_i\right]\\
&+\left[\sum_{k=1}^{\lfloor\kappa_T\rfloor}e^{\frac{\phi}{T^\alpha}k+\frac{\lambda}{T^{\alpha/2}}U_k}\nu_k\right]\left[\sum_{i=\lfloor\kappa_T\rfloor+1}^{T}e^{-\frac{\phi}{T^\alpha}i-\frac{\lambda}{T^{\alpha/2}}U_i}\eta_i\right]\\
&-\sum_{k=1}^{T}\sum_{i=k}^{T}e^{\left(\frac{\phi}{T^\alpha}k+\frac{\lambda}{T^{\alpha/2}}U_k\right)}e^{\left(-\frac{\phi}{T^\alpha}i-\frac{\lambda}{T^{\alpha/2}}U_i\right)}\nu_k\eta_i,
\end{aligned}$$

where we notice that if $\nu_i=\eta_i$ then the latter sum is for $k=1,...T$ and then $i=k+1,...,T$. Given that $T-\lfloor\kappa_T\rfloor=O\left(T^\alpha\right)$, Lemma D.2 implies the first two products are negligible compared to the products with full sums over 1 to T. The third element

can be written

$$\begin{aligned}
&\sum_{k=1}^{T}\sum_{i=k}^{T} e^{\left(\frac{\phi}{T^\alpha}k+\frac{\lambda}{T^{\alpha/2}}U_k\right)}e^{\left(-\frac{\phi}{T^\alpha}i-\frac{\lambda}{T^{\alpha/2}}U_i\right)}\nu_k\eta_i\\
&=\sum_{i=1}^{T}\sum_{k=1}^{i}\left[e^{-\frac{\phi}{T^\alpha}i-\frac{\lambda}{T^{\alpha/2}}U_i}\eta_i\right]e^{\frac{\phi}{T^\alpha}k+\frac{\lambda}{T^{\alpha/2}}U_k}\nu_k\\
&=\sum_{k=1}^{T}\sum_{j=0}^{T-k} e^{-\frac{\phi}{T^\alpha}j-\lambda(U_{k+j}-U_k)}\eta_{k+j}v_k\\
&=O_p\left(\left[T^{\alpha/2}\sum_{k=1}^{T}\nu_k\right]1_{\{\phi>0\}}+\left[T^{\alpha/2}\sum_{k=1}^{T}e^{\left(-\phi+\lambda^2\right)(T-k)/T^\alpha}v_k\right]1_{\{\phi\leq 0\}}\right)\\
&=O_p\left(T^{(1+\alpha)/2}\times 1_{\{\phi>0\}}+T^{\alpha/2}e^{\left(-\phi+\lambda^2\right)T^{1-\alpha}}\times 1_{\{\phi\leq 0\}}\right),
\end{aligned}$$

which proves the required result.

S.3.2.2. Case of R_{0T} By definition and similarly to R^*_{0T}, the remainder R_{0T} can be expressed as: (i) several products that involve sums ranging from $\lfloor\kappa_T\rfloor+1$ to T and which are of lower magnitude since $T-\kappa_T=O\left(T^\alpha\right)$ and all sums diverge; and (ii) the term that needs to be studied, namely

$$\begin{aligned}
&2\left[\sum_{k=1}^{T}e^{\frac{2\phi}{T^\alpha}k+\frac{2\lambda}{T^{\alpha/2}}U_k}\left[\sum_{i=1}^{T}e^{-\frac{\phi}{T^\alpha}i-\frac{\lambda}{T^{\alpha/2}}U_i}\eta_i\right]\sum_{j=k}^{T}\left[e^{-\frac{\phi}{T^\alpha}j-\frac{\lambda}{T^{\alpha/2}}U_j}\eta_j\right]\right]\\
&-\sum_{k=1}^{T}\left(\sum_{i=k}^{T}e^{\frac{\phi}{T^\alpha}k+\frac{\lambda}{T^{\alpha/2}}U_k}\left[e^{-\frac{\phi}{T^\alpha}i-\frac{\lambda}{T^{\alpha/2}}U_i}\eta_i\right]\right)^2\\
&=2R_{2T}-R_{1T}.
\end{aligned}$$

First, we notice that for R_{1T} we can follow the same lines as in the case of R^*_{0T} so

$$\begin{aligned}
R_{1T}&=\sum_{k=1}^{T}\left(\sum_{j=0}^{T-k}e^{-\frac{\phi}{T^\alpha}j-\frac{\lambda}{T^{\alpha/2}}(U_{k+j}-U_k)}\eta_{k+j}\right)^2\\
&=O_p\left(T^{1+\alpha}\times 1_{\{\phi>0\}}+\left[T^\alpha\sum_{k=1}^{T}e^{2\left(-\phi+\lambda^2\right)(T-k)/T^\alpha}\right]1_{\{\phi\leq 0\}}\right)\\
&=O_p\left(T^{1+\alpha}\times 1_{\{\phi>0\}}+\left[T^\alpha e^{2\left(-\phi+\lambda^2\right)T^{1-\alpha}}\right]1_{\{\phi\leq 0\}}\right),
\end{aligned}$$

and $R_{2T} = R_{1T} + \overline{R}_{2T}$, with

$$\begin{aligned}
\overline{R}_{2T} &= \sum_{k=1}^{T} e^{\frac{\phi}{T^\alpha}k + \frac{\lambda}{T^{\alpha/2}}U_k} \\
&\times \sum_{i=1}^{k-1}\left[e^{-\frac{\phi}{T^\alpha}i - \frac{\lambda}{T^{\alpha/2}}U_i}\eta_i\right]\sum_{j=0}^{T-k} e^{-\frac{\phi}{T^\alpha}j - \frac{\lambda}{T^{\alpha/2}}(U_{k+j}-U_k)}\eta_{k+j} \\
&= \sum_{k=1}^{T}\sum_{\ell=1}^{k-1}\left[e^{\frac{\phi}{T^\alpha}\ell + \frac{\lambda}{T^{\alpha/2}}(U_k - U_{k-\ell})}\eta_{k-\ell}\right]\sum_{j=0}^{T-k} e^{-\frac{\phi}{T^\alpha}j - \frac{\lambda}{T^{\alpha/2}}(U_{k+j}-U_k)}\eta_{k+j} \\
&= O_p\left(T^\alpha \sum_k \left[e^{\left(\phi+\lambda^2\right)kT^{-\alpha}}\right]1_{\{\phi>0\}} + \left[e^{\lambda^2 kT^{-\alpha}}e^{\lambda^2(T-k)T^{-\alpha}}\right]1_{\{\phi=0\}}\right. \\
&+ \left.\left[e^{\left(-\phi+\lambda^2\right)(T-k)/T^\alpha}\right]1_{\{\phi<0\}}\right) \\
&= O_p\left(\left[T^\alpha e^{\left(\phi+\lambda^2\right)T^{1-\alpha}}\right]1_{\{\phi>0\}} + \left[T^{1+\alpha}e^{\lambda^2 T^{1-\alpha}}\right]1_{\{\phi=0\}} + \left[T^\alpha e^{\left(-\phi+\lambda^2\right)T^{1-\alpha}}\right]1_{\{\phi<0\}}\right).
\end{aligned}$$

Both magnitudes of R_{1T} and $\overline{R}_{2T}$ are lower than that of S_{1T} so the remainder R_{0T} is asymptotically negligible.

S.3.2.3. Case of $R^{\times}_{0T}$ The proof for $R^{\times}_{0T}$ follows the same line as with R_{0T}, where, we must study now the magnitude of

$$\begin{aligned}
&2\left[\sum_{k=1}^{T} e^{\frac{2\phi}{T^\alpha}k + \frac{2\lambda}{T^{\alpha/2}}U_k}\nu_k\left[\sum_{i=1}^{T} e^{-\frac{\phi}{T^\alpha}i - \frac{\lambda}{T^{\alpha/2}}U_i}\eta_i\right]\sum_{j=k}^{T} e^{-\frac{\phi}{T^\alpha}j - \frac{\lambda}{T^{\alpha/2}}U_j}\eta_j\right] \\
&-\sum_{k=1}^{T}\left(\sum_{i=k}^{T} e^{\frac{\phi}{T^\alpha}k + \frac{\lambda}{T^{\alpha/2}}U_k}\left[e^{-\frac{\phi}{T^\alpha}i - \frac{\lambda}{T^{\alpha/2}}U_i}\eta_i\right]\right)^2\nu_k \\
&= 2R^{\times}_{2T} - R^{\times}_{1T}.
\end{aligned}$$

First, we notice that for $R^{\times}_{1T}$ we can, once again, follow the same lines as in the case of R^{*}_{0T} so

$$\begin{aligned}
R^{\times}_{1T} &= \sum_{k=1}^{T}\left(\sum_{j=0}^{T-k} e^{-\frac{\phi}{T^\alpha}j - \frac{\lambda}{T^{\alpha/2}}(U_{k+j}-U_k)}\eta_{k+j}\right)^2\nu_k \\
&= O_p\left(T^{1/2+\alpha}\times 1_{\{\phi>0\}} + \left[T^\alpha\sum_{k=1}^{T} e^{2\left(-\phi+\lambda^2\right)(T-k)/T^\alpha}\nu_k\right]1_{\{\phi\leq 0\}}\right) \\
&= O_p\left(T^{1/2+\alpha}\times 1_{\{\phi>0\}} + \left[T^\alpha e^{2\left(-\phi+\lambda^2\right)T^{1-\alpha}}\right]1_{\{\phi\leq 0\}}\right),
\end{aligned}$$

and $R_{2T}^{\times} = R_{1T}^{\times} + \overline{R}_{2T}^{\times}$, with

$$\begin{aligned}
\overline{R}_{2T}^{\times} &= \sum_{k=1}^{T} e^{\frac{\phi}{T^{\alpha}}k + \frac{\lambda}{T^{\alpha/2}}U_k}\nu_k \\
&\quad \times \sum_{i=1}^{k-1}\left[e^{-\frac{\phi}{T^{\alpha}}i - \frac{\lambda}{T^{\alpha/2}}U_i}\eta_i\right]\sum_{j=0}^{T-k} e^{-\frac{\phi}{T^{\alpha}}j - \frac{\lambda}{T^{\alpha/2}}(U_{k+j}-U_k)}\eta_{k+j} \\
&= \sum_{k=1}^{T}\nu_k \sum_{\ell=1}^{k-1}\left[e^{\frac{\phi}{T^{\alpha}}\ell + \frac{\lambda}{T^{\alpha/2}}(U_k - U_{k-\ell})}\eta_{k-\ell}\right]\sum_{j=0}^{T-k} e^{-\frac{\phi}{T^{\alpha}}j - \frac{\lambda}{T^{\alpha/2}}(U_{k+j}-U_k)}\eta_{k+j} \\
&= O_p\left(T^{\alpha}\sum_{k}\left[e^{\left(\phi+\lambda^2\right)kT^{-\alpha}}\nu_k\right]1_{\{\phi>0\}} + \left[e^{\lambda^2 kT^{-\alpha}}e^{\lambda^2(T-k)T^{-\alpha}}\nu_k\right]1_{\{\phi=0\}}\right. \\
&\quad \left. + \left[e^{\left(-\phi+\lambda^2\right)(T-k)/T^{\alpha}}\nu_k\right]1_{\{\phi<0\}}\right) \\
&= O_p\left(\left[T^{\alpha}e^{\left(\phi+\lambda^2\right)T^{1-\alpha}}\right]1_{\{\phi>0\}} + \left[T^{1/2+\alpha}e^{\lambda^2 T^{1-\alpha}}\right]1_{\{\phi=0\}} + \left[T^{\alpha}e^{\left(-\phi+\lambda^2\right)T^{1-\alpha}}\right]1_{\{\phi<0\}}\right),
\end{aligned}$$

which is the required result.

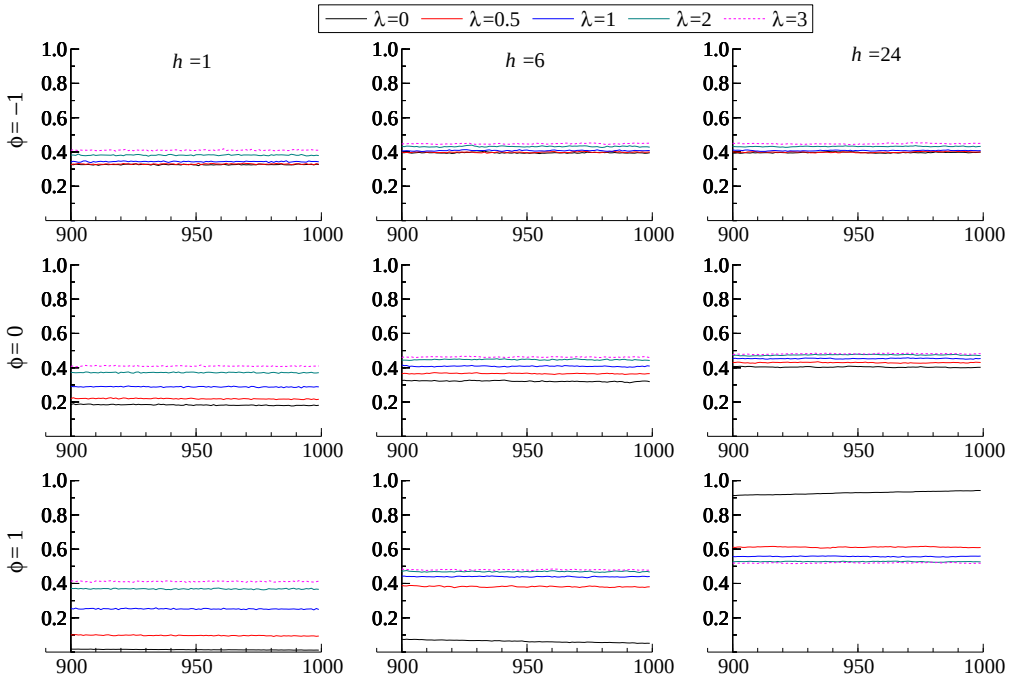

Figure S.1. The figure records simulated probabilities $\pi_{t,h}(\gamma)$ for $\gamma = 1.05$ and $900 \leq t \leq 1000$ and $\alpha = .8$. Each row records a different value of $\phi \in \{-1, 0, 1\}$, and each column a value of the horizon $h \in \{1, 6, 24\}$; the graphs record different values of $\lambda \in \{0, .5, 1, 2, 3\}$. The number of Monte Carlo replications is 5×10^4.

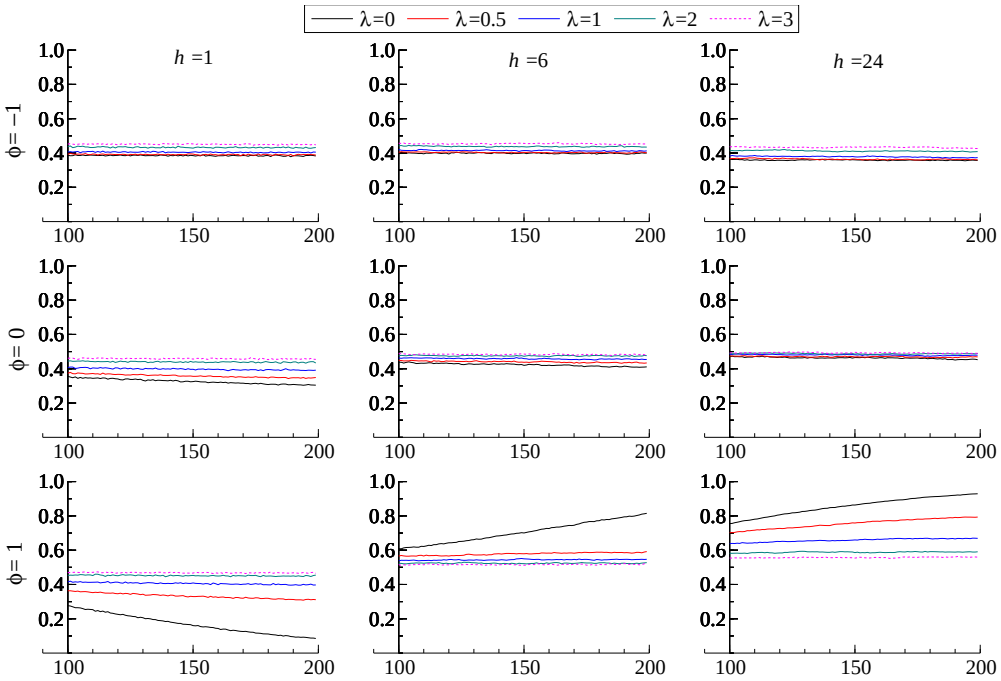

Figure S.2. The figure records simulated probabilities $\pi_{t,h}(\gamma)$ for $\gamma = 1.05$, $100 \leq t \leq 200$ and $\alpha = .8$. Each row records a different value of $\phi \in \{-1, 0, 1\}$, and each column a value of the horizon $h \in \{1, 6, 24\}$; the graphs record different values of $\lambda \in \{0, .5, 1, 2, 3\}$. The number of Monte Carlo replications is 5×10^4.

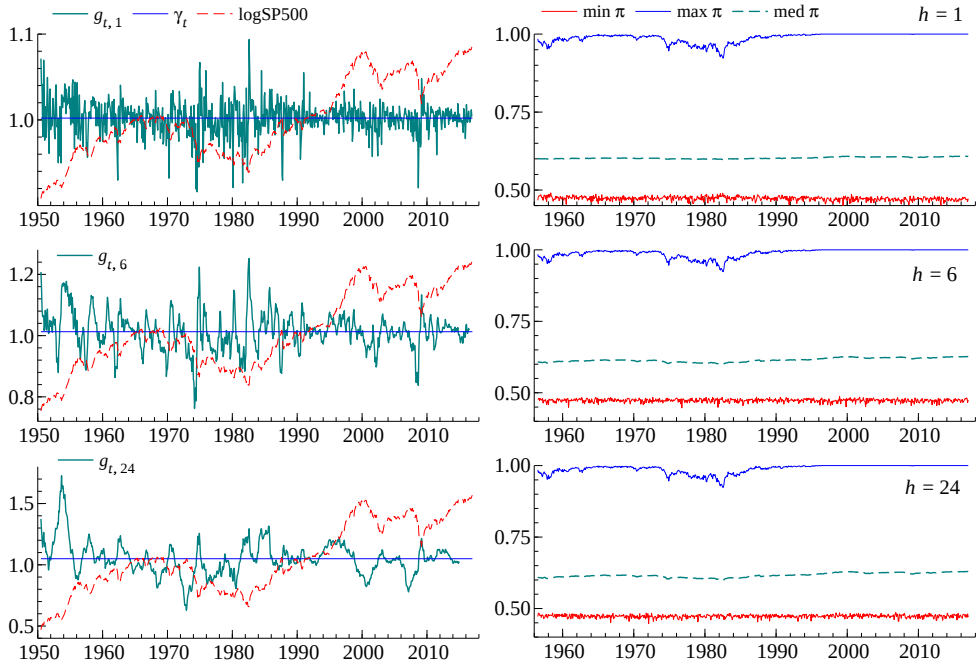

Figure S.3. Predictive probabilities for the logarithm of the monthly S&P 500 stock index. The left column reports the actual series as well as the growth $g_{t,h} = y_{t+h}/y_t$ for horizons $h = 1, 6$ and 24 in, respectively, the top, middle and bottom rows. The log price data are scaled to match the mean and range of $g_{t,h}$. The benchmark γ_t for computing probabilities is set to 1.004 for all horizons. The right-hand side column reports probabilities $\widehat{\pi}_{t,h}^{\min}(\gamma_t)$, $\widehat{\pi}_{t,h}^{\max}(\gamma_t)$ and $\widehat{\pi}_{t,h}^{med}(\gamma_t)$. Minimum and maximum are computed over the set of parameters which are not rejected at a nominal size of 0.10.

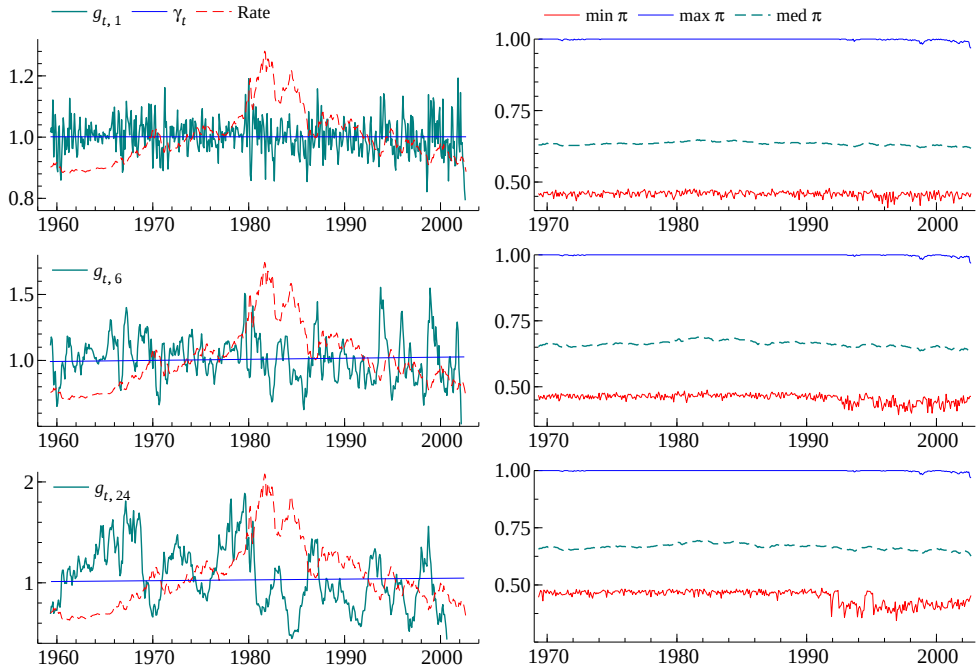

Figure S.4. Predictive probabilities for the U.S. monthly long run interest rate. The left column reports the actual series as well as the growth $g_{t,h} = y_{t+h}/y_t$ for horizons $h = 1, 6$ and 24 in, respectively, the top, middle and bottom rows. The interest rate data are scaled to match the mean and range of $g_{t,h}$. The benchmark γ_t for computing probabilities is set to 1 for all horizons. The right-hand side column reports probabilities $\widehat{\pi}^{\min}_{t,h}(\gamma_t)$, $\widehat{\pi}^{\max}_{t,h}(\gamma_t)$ and $\widehat{\pi}^{med}_{t,h}(\gamma_t)$. Minimum and maximum are computed over the set of parameters which are not rejected at a nominal size of 0.10.